

## Interlayer conductivity in the superconductor $\text{Tl}_2\text{Ba}_2\text{CuO}_{6+\delta}$ : Energetics and energy scales

A. S. Katz, S. I. Woods, and E. J. Singley

*Department of Physics, University of California—San Diego, La Jolla, California 92093-0319*

T. W. Li\*

*Department of Materials Science, Argonne National Laboratory, Argonne, Illinois 60439*

M. Xu\*

*James Franck Institute, University of Chicago, Chicago, Illinois 60637*

D. G. Hinks

*Department of Materials Science, Argonne National Laboratory, Argonne, Illinois 60439*

R. C. Dynes and D. N. Basov

*Department of Physics, University of California—San Diego, La Jolla, California 92093-0319*

(Received 13 October 1999)

We report on infrared studies of the  $c$ -axis electrodynamics of  $\text{Tl}_2\text{Ba}_2\text{CuO}_{6+\delta}$  crystals. A sum-rule analysis reveals spectral weight shifts that can be interpreted as a kinetic energy change at the superconducting transition. In optimally doped crystals, showing an incoherent normal-state response, the kinetic energy is lowered at  $T < T_c$ , but no significant change is found in the overdoped samples, which have more coherent conductivity at  $T > T_c$ .

Despite extensive experimental effort in high- $T_c$  superconductivity over the last decade very little is known about the microscopic roots of the condensation energy,  $E_c$ , in this class of materials. In conventional superconducting metals  $E_c$  is due to the *reduction* of the potential energy, which overwhelms the *increase* of the electronic kinetic energy.<sup>1</sup> Several models of high- $T_c$  superconductivity propose entirely different energetics of  $E_c$  with the superconducting state being driven by changes of the Coulomb energy,<sup>2</sup> exchange energy<sup>3,4</sup> or kinetic energy.<sup>5–9</sup> Existing experimental results are inconclusive.<sup>10–12,3</sup>

A variety of models enable inference of the electronic kinetic energy from a sum-rule analysis of the complex optical conductivity  $\sigma(\omega) = \sigma_1(\omega) + i\sigma_2(\omega)$ .<sup>13</sup> A partial sum rule relates the integral of  $\sigma_1(\omega)$  over a limited energy range  $W$  to the kinetic energy  $-\alpha$ :

$$\int_0^W d\omega \sigma_1(\omega) = -\alpha. \quad (1)$$

For the case of a superconductor Eq. (1) can be rephrased in the form of a modified Ferrel-Glover-Tinkham (FGT) sum rule to yield the kinetic energy sum rule:<sup>7,8,14</sup>

$$\rho_s = [N_n - N_s] + [\alpha_n - \alpha_s]. \quad (2)$$

In Eq. (2),  $\rho_s$  is the superfluid density that quantifies the spectral weight under the superconducting  $\delta$  function.<sup>15</sup> Integrals  $N_n(\omega) = (120/\pi) \int_0^\omega d\omega' \sigma_1(\omega', T > T_c)$  and  $N_s(\omega) = (120/\pi) \int_0^\omega d\omega' \sigma_1(\omega', T \leq T_c)$  are proportional to the number of carriers participating in absorption above and below  $T_c$ . The magnitude of  $\rho_s = 4\pi\omega\sigma_2(\omega \rightarrow 0)$  and  $[N_n - N_s]$  are obtained independently from the optical constants.<sup>12</sup> Typically, the  $[N_n - N_s]$  integrals converge at energies below  $10\text{--}15 k_B T_c$ .<sup>16</sup> A comparison of the magni-

tudes of  $\rho_s$  and  $[N_n - N_s]$  then provides a basis for an experimental probe of the kinetic energy change  $\Delta\alpha = [\alpha_n - \alpha_s]$ . Physically, the nonvanishing magnitude of  $\Delta\alpha$  implies that changes of the low-energy spectral weight in Eq. (1) are compensated by readjustment of interband transitions at  $\omega > W$  so that the global sum rule  $\int_0^\infty d\omega \sigma_1(\omega) = \pi n e^2 / 2m_e$  is satisfied.

Recently, we found a  $\rho_s > [N_n - N_s]$  inequality in the interlayer conductivity of a variety of cuprates indicating that the superconducting condensate is collected from an interband-scale energy range.<sup>12</sup> This result can be interpreted in terms of a reduction of the kinetic energy below  $T_c$ . In this paper we explore the connection between the development of coherence in the interlayer conductivity and the anomalous behavior of the  $c$ -axis superconducting condensate in  $\text{Tl}_2\text{Ba}_2\text{CuO}_{6+\delta}$  (Tl-2201). We found that the energy scale associated with superconductivity extended to the interband region when the normal-state conductivity across the layers was nearly blocked. Once the interlayer transport above  $T_c$  became more coherent, the FGT sum rule approached exhaustion at energies below  $\sim 5 k_B T_c$  suggesting that any kinetic energy change was very small or nonexistent.

$\text{Tl}_2\text{Ba}_2\text{CuO}_{6+\delta}$  is an ideal material for studying the overdoped regime of the phase diagram in which a variety of cuprates reveal a crossover to a more coherent response. Highly overdoped crystals of Tl-2201 have nearly identical chemical composition to the optimally doped phase since less than 2% change in the oxygen content is required to suppress  $T_c$  from the maximum value of  $T_c \approx 90$  K down to less than 4 K.<sup>17,18</sup> Crystal preparation is described elsewhere.<sup>10</sup> Typical crystal dimensions were nominally  $0.8 \text{ mm} \times 0.8 \text{ mm} \times 0.08 \text{ mm}$ . Mosaics of several specimens with similar  $T_c$  and  $\Delta T_c$  (determined from magnetization measurements) were prepared and polished along a face par-

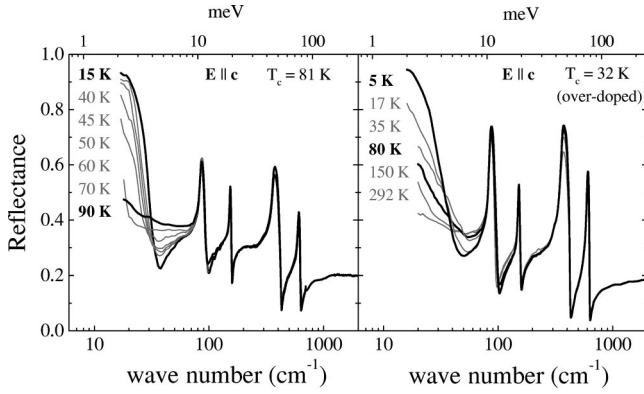


FIG. 1. Reflectance of TI-2201 measured with  $E||c$  polarization of incident radiation. Left panel: The optimally doped sample develops a superconducting plasma edge out of an apparently insulating spectrum for  $T < T_c$ . Right panel: The over-doped sample shows continuously increasing reflectance above and below  $T_c$ .

allel to the  $c$  axis. The polished surfaces were smooth, black, and shiny. Infrared reflectance,  $R_c(\omega)$ , was measured with  $E||c$  polarized light in the frequency range from 16 to 15 000  $\text{cm}^{-1}$  using a spectrometer configured for microsamples. Spectra taken at different temperatures had a relative experimental uncertainty of less than 0.5%.

In Fig. 1, we show the raw reflectance results for the optimally and overdoped crystals. The  $E||c$  reflectance of both samples over the range of 80–2000  $\text{cm}^{-1}$  (10–250 meV) resembled an ionic insulator with a low reflectivity punctuated by phonon peaks. Both samples showed a plasma edge below  $T_c$ . Classical electrodynamics describes the development of this plasma edge since superconducting currents flow along all crystallographic directions.<sup>19</sup> In the optimally doped sample ( $T_c = 81$  K,  $\Delta T_c \approx 8$  to 10 K) the plasma edge grew out of an apparently insulating normal-state spectrum. In the overdoped sample ( $T_c = 32$  K,  $\Delta T_c \approx 5$  K) we found a “metallic” up-turn in  $R_c(\omega)$  measured above  $T_c$ , consistent with more coherent delocalized behavior. Below  $T_c$ , the reflectance continued to rise, and the plasma edge developed a characteristic minimum at a frequency position of  $\omega = 49$   $\text{cm}^{-1}$ . The minimum in reflectance was shifted to higher frequencies compared to  $\omega = 37$   $\text{cm}^{-1}$  in the optimally doped case.

The raw  $E||c$  reflectance data was transformed using the Kramers-Kronig relations to determine the complex conductivity. Extrapolations of the reflectance data to low and high frequencies, required for the Kramers-Kronig integrals, did not strongly affect the results in the frequency range where measured data exists. The real part of the conductivity spectra were dominated by strong phonon peaks (Fig. 2). Three of the modes at 85, 151, and 360  $\text{cm}^{-1}$  were unaffected by doping; the highest frequency mode softened from 602  $\text{cm}^{-1}$  in the optimally doped crystal down to 595  $\text{cm}^{-1}$  in the overdoped sample. The electronic background of the conductivity of the optimally doped sample was nearly flat and featureless for temperatures above and below  $T_c$ . The response of the overdoped crystal was different. The conductivity below 80  $\text{cm}^{-1}$  showed a Drude-like behavior steadily rising out of a  $\sim 5$  ( $\Omega\text{cm})^{-1}$  background. Below  $T_c$ , this “metal-

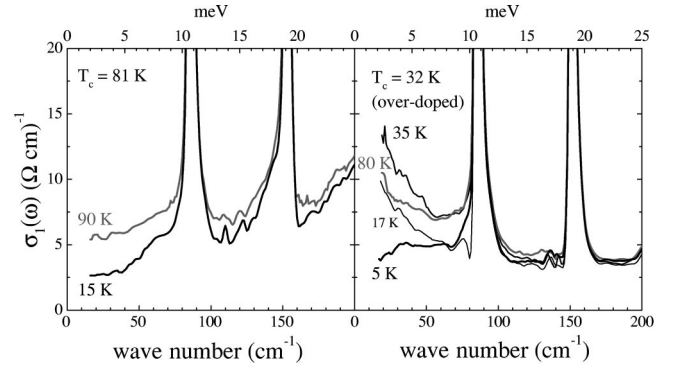


FIG. 2. Real part of the complex conductivity of TI-2201 calculated from the reflectivity shown in Fig. 1. Left panel: The conductivity of the optimally doped sample is punctuated by phonon peaks but is otherwise nearly flat and featureless. Right panel: The over-doped sample shows the same phonon peaks but develops a coherent, Drude-like peak for  $T > T_c$  that condenses into the superfluid condensate when  $T < T_c$ .

lic” response diminished as temperature was lowered. By  $T = 5$  K, it effectively vanished, and the conductivity (ignoring phonon peaks) was nearly frequency independent. Just above  $T_c$ , the dc conductivity of the over-doped sample at  $T = 35$  K [obtained from the extrapolation of  $\sigma_1(\omega)$  to  $\omega = 0$ ] was  $\sim 15$  ( $\Omega\text{cm})^{-1}$ . This is roughly a factor of 3 higher than the value obtained for optimally doped TI-2201 crystals. It has been established that increasing oxygen content causes the  $c$  axis to contract.<sup>20</sup> This closer spacing of the  $\text{CuO}_2$  planes favors enhanced interlayer coupling and likely leads to the more coherent behavior of the conductivity. It is important to emphasize, however, that the  $c$ -axis conductivity is still two orders of magnitude smaller than the in-plane dc conductivity, and it is 4–6 orders of magnitude smaller than the conductivity of conventional metals.

Using the complex conductivity spectra above and below  $T_c$ , we can identify the spectral origins of the superfluid condensate. In all of our measurements, the conductivity at  $T < T_c$  was suppressed compared to spectra taken at  $T \approx T_c$ , but we saw no evidence of a classical superconducting gap  $\Delta$  for  $T \ll T_c$ . The absolute value of  $\sigma_1(\omega)$  persisted well above the noise level down to the lowest measured frequencies, behavior consistent with gaplessness. To quantify the transfer of spectral weight below  $T_c$ , we plotted the ratio  $[N_n(\omega) - N_s(\omega)]/\rho_s$  as a function of  $\omega$  in Fig. 3.<sup>12</sup> The superfluid density  $\rho_s$  was determined from the extrapolation of  $\omega\sigma_2(\omega, T)$  to  $\omega = 0$  for  $T \ll T_c$ , a procedure that does not require model-dependent assumptions.<sup>21</sup> The frequency dependence of  $[N_n(\omega) - N_s(\omega)]/\rho_s$  unfolds the sum-rule integrals. In the optimally doped sample, the ratio rose slowly and saturated near a value of about 0.6 at  $\omega \approx 30$ –40 meV. The energy interval in Fig. 3 corresponds to  $\sim 22 k_B T_c$ , more than sufficient for the conventional FGT sum rule. The data for the optimally doped sample implied that a significant portion of  $\rho_s$  was accumulated from energies above 0.15 eV. In contrast, in overdoped TI-2201 the dominant fraction of the superfluid density was collected from the far-infrared, low-energy region. Within our experimental uncertainty, at least 80–90% of  $\rho_s$  was accumulated from energies as small as 4–5  $k_B T_c$ .<sup>22</sup> The error bars shown in Fig. 3 were determined by varying the high- and low-frequency extrapolations

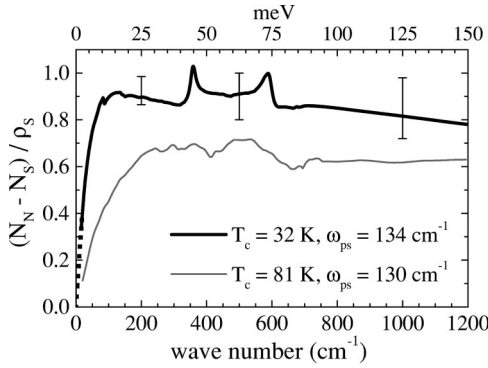


FIG. 3. The ratio of the spectral weight difference  $[N_n(\omega) - N_s(\omega)]$  to the superfluid density  $\rho_s$  as described in the text for optimally ( $T_c = 81$  K) and over doped ( $T_c = 32$  K) TI-2201. The superfluid condensate is accumulated from lower energies in the overdoped sample. To calculate the overdoped curve, we extrapolated (shown as a dashed line)  $\sigma_1(\omega, T = 35$  K) from  $\omega = 16$   $\text{cm}^{-1}$  to  $\omega = 0$  using a Drude function with  $\sigma_{dc} = 15$  ( $\Omega \text{ cm}^{-1}$ ) $^{-1}$  and  $\tau^{-1} = 45$   $\text{s}^{-1}$ , and  $\sigma_1(\omega, T = 5$  K) = 5 ( $\Omega \text{ cm}^{-1}$ ) $^{-1}$ .

to the data and by allowing for constant offsets of  $R(\omega)$  within our signal-to-noise ratio. Comparison of the data plotted in Figs. 2 and 3 suggests that the behavior of the conductivity above  $T_c$  determines the energy scales from which the superconducting condensate is collected. In the case of the overdoped crystal there is no need to extend integration of the conductivity to midinfrared and near-infrared energies in order to account for the magnitude of  $\rho_s$  since the required spectral weight is readily available at low energies.

If Eq. (2) is chosen as the basis for data interpretation, then the  $\rho_s > [N_n - N_s]$  inequality observed in the optimally doped crystal implies a reduction of the electronic kinetic energy below  $T_c$ . The reduction of the kinetic energy can be understood by noting that the charge carriers are nearly confined to the  $\text{CuO}_2$  planes above  $T_c$  whereas in the superconducting state *paired* charges move more easily between the layers. On the contrary, the overdoped sample, which revealed a more coherent *c*-axis response [Drude-like upturn of  $\sigma_1(\omega)$  and enhanced dc conductivity], showed  $\Delta\alpha \approx 0$  within our error bars. The data suggested that a kinetic energy change is observed only if deconfinement of the charge carriers occurs by virtue of pair tunneling below  $T_c$ . If the charge carriers were already delocalized in the normal state (even with very low plasma frequencies), then the magnitude of  $\Delta\alpha$  is vanishingly small. The same trend was observed in the *c*-axis response of the  $\text{YBa}_2\text{Cu}_3\text{O}_x$  (YBCO) family. The discrepancy between  $[N_n(\omega) - N_s(\omega)]$  and  $\rho_s$ , suggesting a lowering of the kinetic energy, was most extreme in  $\text{YBa}_2\text{Cu}_3\text{O}_{6.53}$ . As the oxygen content was raised, the excess spectral weight appeared in the lower energy part of  $\sigma_1(\omega, T > T_c)$  spectra. The  $[N_n(\omega) - N_s(\omega)]/\rho_s$  ratio with integration limited up to 10–15  $k_B T_c$  was near unity for  $\text{YBa}_2\text{Cu}_3\text{O}_{6.85}$  and higher doping levels indicating that  $\Delta\alpha$  became vanishingly small.<sup>23</sup>

Further analysis of the overdoped TI-2201 crystal showed a lower energy scale associated with superconductivity. It has been experimentally observed in a wide variety of cu-

prates that the magnitude of the *c*-axis penetration depth  $\lambda_c = c/\sqrt{\rho_s}$  is related to the dc conductivity  $\sigma_{dc}$  at  $T \approx T_c$  by the relationship

$$\lambda_c^{-2} = \frac{1}{\hbar c^2} \Omega_S \sigma_{dc}(T \approx T_c), \quad (3)$$

where  $\Omega_S$  is an energy scale associated with superconductivity.<sup>24–26,8</sup> Equation (3) may be obtained either by modeling a dirty-limit bulk superconductor or by treating the anisotropic cuprates as a weakly coupled stack of intrinsic Josephson junctions. Those models find  $\Omega_S = 4\pi^2\Delta$ . In our experiments,  $\lambda_c$  remained nearly unchanged<sup>21</sup> whereas the *c*-axis dc conductivity increased by a factor of  $\sim 3$  in the overdoped crystals. If Eq. (3) holds true, then  $\Omega_S$  must be reduced in the overdoped regime in order to keep the penetration depth constant. Supporting evidence that  $\Omega_S$  is indeed reduced for overdoped TI-2201 comes from Raman-scattering measurements on optimally and overdoped TI-2201 which found that a spectral feature attributed to the superconducting energy gap  $2\Delta$  shifted down in frequency from  $\sim 350$   $\text{cm}^{-1}$  in optimally doped TI-2201 to  $\sim 105$   $\text{cm}^{-1}$  in an overdoped sample as  $T_c$  fell from 78 to 37 K.<sup>27,28</sup> *c*-axis polarized Raman scattering in  $\text{Bi}_2\text{Sr}_2\text{CaCu}_2\text{O}_{8+\delta}$  (Bi-2212) single crystals also showed an energy scale that diminished in overdoped samples.<sup>29</sup> The lower energy scale of the superfluid condensation seen in Fig. 3 is consistent with a reduction in  $\Omega_S$ .<sup>30</sup>

Several important distinctions of overdoped phases from the optimally doped counterparts have been observed in different families of the cuprates. Raman spectroscopy showed both in TI-2201 and Bi-2212 single crystals highly anisotropic energy gaps at optimal doping but revealed behavior interpreted as a crossover to a more isotropic behavior in overdoped samples.<sup>27,31</sup> This is consistent with the results of angular-resolved photoemission (ARPES) on Bi-2212.<sup>32</sup> Thus, both Raman and ARPES studies suggested a trend towards the development of a more isotropic superconducting state in overdoped crystals. We observed a more conventional superfluid response in overdoped TI-2201 compared to the optimally doped sample. Phase sensitive measurements of the order parameter in overdoped materials are needed to determine if the above observations are associated with the development of an *s* component of the order parameter. An *s*-wave component in the order parameter in the overdoped regime is possible within the stripe-based models.<sup>9</sup>

In conclusion, we employed infrared spectroscopy to examine the energy scales of the superconducting state in TI-2201. We found that the superfluid spectral weight was accumulated from lower energies when the *c*-axis conductivity showed a more coherent, delocalized response. Using the modified FGT sum rule we could extract kinetic energy changes and correlate these changes to the normal-state *c*-axis conductivity.

We thank D. A. Kossenko for technical assistance. Work at UCSD was supported by NSF Grant No. DMR-9875980, AFOSR Grant No. F4962-098-0264, the Sloan Foundation, and the Research Corporation. Work at Argonne was supported by NSF Grant No. DMR 91-20000 and by DOE Contract No. W-31-109-ENG-38.

- \*Present address: Lucent Technologies, 2000 North Naperville Road, Naperville, IL 60566.
- <sup>1</sup>M. Tinkham, *Introduction to Superconductivity* (McGraw-Hill, New York, 1994).
  - <sup>2</sup>A.J. Leggett, *J. Phys. Chem. Solids* **59**, 1729 (1998).
  - <sup>3</sup>E. Demler and S.-C. Zhang, *Nature (London)* **396**, 733 (1998).
  - <sup>4</sup>D.J. Scalapino and S.R. White, *Phys. Rev. B* **58**, 8222 (1998).
  - <sup>5</sup>J.E. Hirsch, *Phys. Rev. Lett.* **59**, 228 (1987).
  - <sup>6</sup>P.W. Anderson, *The Theory of Superconductivity in the High- $T_c$  Cuprates* (Princeton University Press, Princeton, NJ, 1998); *Science* **279**, 1196 (1998).
  - <sup>7</sup>J.E. Hirsch, *Physica C* **199**, 305 (1992).
  - <sup>8</sup>S. Chakravarty, *Eur. Phys. J. B* **5**, 337 (1998); S. Chakravarty, H.-Y. Kee, and E. Abrahams, *Phys. Rev. Lett.* **82**, 2366 (1999).
  - <sup>9</sup>V.J Emery and S.A. Kivelson, cond-mat/9809083 (unpublished).
  - <sup>10</sup>K.A. Moler *et al.*, *Science* **279**, 1193 (1998).
  - <sup>11</sup>A.A. Tsvetkov *et al.*, *Nature (London)* **395**, 360 (1998).
  - <sup>12</sup>D.N. Basov *et al.*, *Science* **283**, 49 (1999).
  - <sup>13</sup>P.F. Maldague, *Phys. Rev. B* **16**, 2437 (1977); B.S. Shastry and B. Sutherland, *Phys. Rev. Lett.* **65**, 243 (1990); M.V. Klein and G. Blumberg, *Science* **283**, 42 (1999).
  - <sup>14</sup>E.H. Kim, *Phys. Rev. B* **58**, 2452 (1998).
  - <sup>15</sup>We define  $\rho_s = 4\pi e^2 n_s / m^*$ , where  $e$  is the electron charge,  $n_s$  is the density of superconducting carriers, and  $m^*$  is their mass. This definition implies  $\rho_s$  has dimensions of the plasma frequency squared ( $\text{cm}^{-2}$ ).
  - <sup>16</sup>The energy scale of the order of  $15 kT_c$  is sufficient to satisfy the FGT sum rule in the case of  $ab$ -plane conductivity of most cuprates, including optimally doped Tl-2201 [Z. Schlesinger *et al.*, *Phys. Rev. B* **41**, 11 237 (1990); D.N. Basov *et al.*, *Phys. Rev. Lett.* **74**, 598 (1995); A.V. Puchkov *et al.*, *Phys. Rev. B* **51**, 3312 (1995)].
  - <sup>17</sup>Y. Kubo *et al.*, *Phys. Rev. B* **43**, 7875 (1991).
  - <sup>18</sup>T. Manako *et al.*, *Physica C* **185-189**, 1327 (1991).
  - <sup>19</sup>J. Schutzmann *et al.*, *Phys. Rev. B* **55**, 11 118 (1997).
  - <sup>20</sup>C. Opagiste *et al.*, *Physica C* **213**, 17 (1993); C.A. Wang *et al.*, *ibid.* **262**, 98 (1996).
  - <sup>21</sup>We obtained a value for the superconducting plasma frequency,  $\omega_{ps} = \sqrt{\rho_s} = 134 \pm 5 \text{ cm}^{-1}$ , and the  $c$ -axis penetration depth,  $\lambda_c = c/\sqrt{\rho_s} = 11.5 \pm 0.5 \mu\text{m}$ . These are nearly the same values obtained for optimally doped Tl-2201 ( $\omega_{ps} = 130 \text{ cm}^{-1}$ ,  $\lambda_c = 12 \mu\text{m}$ ). Moler *et al.* (unpublished) also observed that the  $c$ -axis penetration depths of optimally and overdoped Tl-2201 crystals are nearly equal, although their values were about 20% larger.
  - <sup>22</sup>The peaks at approximately 45 and 75 meV in the overdoped sample data in Fig. 3 are due to the slight temperature dependence of unextracted  $c$ -axis phonons. The phonons have been removed in the optimally doped data since they showed a much stronger temperature dependence. Data with phonons can be found in Ref. 12.
  - <sup>23</sup>D.N. Basov (unpublished).
  - <sup>24</sup>D.N. Basov *et al.*, *Phys. Rev. B* **50**, 3511 (1994).
  - <sup>25</sup>S. Uchida and K. Tamasaku, *Physica C* **293**, 1 (1997).
  - <sup>26</sup>J.R. Kirtley, K.A. Moler, G. Villard, and A. Maignan, *Phys. Rev. Lett.* **81**, 2140 (1998).
  - <sup>27</sup>C. Kendziora, R.J. Kelley, and M. Onellion, *Phys. Rev. Lett.* **77**, 727 (1996).
  - <sup>28</sup>M. Kang *et al.*, *Phys. Rev. Lett.* **77**, 4434 (1996).
  - <sup>29</sup>H.L. Liu *et al.*, *Phys. Rev. Lett.* **82**, 3524 (1999).
  - <sup>30</sup>Data shown in Fig. 3 suggested a stronger suppression of the energy scale from which the condensate is collected than a factor of 3 inferred from Eq. (3). This equation implies that the entire spectral weight contained in the normal state conductivity at  $\omega < \Omega_S$  is transferred to the  $\delta$  function in the superconducting state. This is a correct assumption for a BCS superconductor, but in cuprates only a small fraction of the normal-state spectral weight goes into the condensate (see Fig. 2).
  - <sup>31</sup>This interpretation of Raman data is not exclusive. For other interpretations, see L.V. Gasparov *et al.*, *Phys. Rev. B* **58**, 11 753 (1998); K.C. Hewitt *et al.*, *Phys. Rev. Lett.* **78**, 4891 (1997); C. Kendziora and M. Onellion, *ibid.* **78**, 4892 (1997).
  - <sup>32</sup>R.J. Kelley *et al.*, *Science* **271**, 1255 (1996).